Structural requirements of non-peptide neurotensin receptor antagonists

Luc Quéré,[a] Robert Boigegrain,[b] Francis Jeanjean,[b] Danielle Gully,[c] Guy Evrard[a] and François Durant[a]

[a] *Laboratoire de Chimie Moléculaire Structurale, Facultés Universitaires Notre-Dame de la Paix, Rue de Bruxelles 61, B5000 Namur, Belgium*
[b] *Sanofi Recherche, Neuropsychiatry Department, 371 rue du Pr. Blayac 34184 Montpellier Cedex 04, France*
[c] *Sanofi Recherche, 195 route d'Espagne, 31000 Toulouse, France*

Neurotensin has a wide range of pharmacological effects in peripheral tissues and in the central nervous system. The crystal structures of two potent and selective neurotensin receptor antagonists, SR 48692 (I) and SR 48527 (II) have been determined and are reported in this work. By using computational calculations (semiempirical molecular orbital AM1) we studied the conformational properties of those compounds, including an inactive analogue SR 49711 (III) for comparison. Considering the pharmacological properties related to SR 48692 (I) and to optically synthetic analogues SR 48527 (II) and SR 49711 (III), we propose a model of bioactive conformation adopted by those neurotensin receptor antagonists.

Neurotensin (NT) is a 13 amino acid peptide (pGlu-Leu-Tyr-Glu-Asn-Lys-Pro-Arg-Arg-Pro-Tyr-Ile-Leu) which was first isolated from bovine hypothalamus.[1] It was subsequently demonstrated that it is also present in specific regions of the central nervous system, the pituitary and the gastrointestinal tract of a variety of species including man.[2–4] Neurotensin has a wide range of pharmacological effects in peripheral tissues and in the central nervous system.[5] It acts as a neuromodulator in the brain and as a gastrointestinal hormone in the periphery. Concerning its neuromodulatory role, the possibility of a subtle and complex modulation of the dopaminergic system offers the exciting possibility of a new treatment strategy for psychotic disorders.[6–9]

In the last few years, the discovery of a number of NT antagonists has been reported.[10] In the course of screening to discover non-peptide receptor antagonists, compound **I**

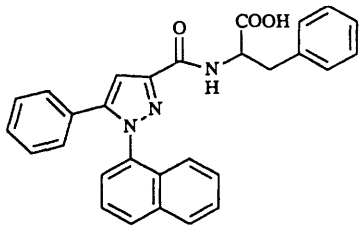

SR 45398

(SR 48692), 2-{[1-(7-chloroquinolin-4-yl)-5-(2,6-dimethoxyphenyl)-1*H*-pyrazol-3-ylcarbonyl]amino}adamantane-2-carboxylic acid was reported as the first non-peptide antagonist of the NT receptor in tissues of various species including man.[11] It was obtained by the optimization of a lead compound, SR 45398 discovered by random screening of several thousand compounds. Systematic structural modifications of this molecule revealed the importance of 2,6-dimethoxy substitutions in the phenyl ring in position 5 of the pyrazole ring. A large aromatic group in position 1 and an amino acid linked by means of its amino group to a carbonyl in position 3 of the pyrazole ring are also important features for a full receptor binding.[12]

Structure–affinity studies reveal that the C$^{\alpha}$ carbon atom of the terminal amino acid has to have a free carboxylic acid and

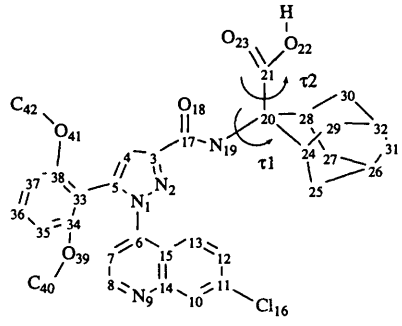

I (SR 48692)

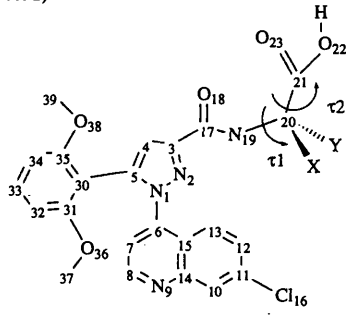

II (SR 48527)	X= H	Y= 
III (SR 49711)	X= 	Y= H

Scheme 1

a bulky lipophilic group.[13] At this level, substitution of the C$^{\alpha}$ carbon atom with a cyclohexyl group, for example, creates an asymmetric centre which can discriminate between active and inactive compounds. In this case, the compound **II** (SR 48527), (*S*)-(+)-{[1-(7-chloroquinolin-4-yl)-5-(2,6-dimethoxyphenyl)-1*H*-pyrazol-3-ylcarbonyl]amino}-cyclohexylacetic acid, is a

much more potent antagonist than the *R* enantiomer SR 49711 (**III**) (Table 1).[14] However, SR 48692 (**I**), which does not contain any chiral centre, but a 2-amino-adamantane-2-carboxylic acid group as terminal chain, is likewise a very good candidate for the binding to NT receptor (Table 1).

In order to characterize the structural requirements of such NT antagonists, we analysed the crystal structures of two potent and selective non-peptide antagonists **I** (SR 48692) and **II** (SR 48527). The present work details the conformational properties determined by X-ray diffraction and the geometric analysis of the crystal packing. Starting from the crystallographic data, we scanned the conformational space around the flexible bonds of the molecules. For this purpose, we used AM1 molecular orbital calculations. In the same manner, we studied the conformational properties of the inactive enantiomer **III** (SR 49711). Considering together the structural properties and the pharmacological data, we propose in this work a bioactive conformational model for those neurotensin receptor antagonists.

Table 1 Inhibition of [^{125}I]neurotensin specific binding to adult guinea-pig brain membranes (method described in Experimental section; K_i values were determined according to Cheng and Prusoff.[12] n_H: Hill coefficients. Each value is the mean ± sem of at least three experiments)

Compound	K_i (nmol dm^{-3})	n_H
I	3.5 ± 0.2	0.96 ± 0.03
II	6.2 ± 0.6	1.06 ± 0.20
III	318 ± 92	0.94 ± 0.1

Results and discussion

Structural analysis of I

Single-crystal structure of I. The crystal conformation and crystal packing of compound **I** are shown in Fig. 1. Relevant bond lengths and torsion angles are presented in Table 2.

The N(1)–C(6) bond length, 1.433(6) Å, which connects the quinoline group to the pyrazole ring is significantly longer than expected for a standard N(sp^2)–C(sp^2) bond (1.339 Å). Such a bond length indicates the absence of any significant orbital overlap.[15] Due to steric hindrance, the quinoline moiety is almost perpendicular to the pyrazole ring [N(2)–N(1)–C(6)–C(7) = 67.3(7)°]. The 2,6-dimethoxyphenyl group shows a similar pattern: a bond length C(5)–C(33) of 1.484(7) Å between the two aromatic rings, and a torsion angle value of 64.8(7)° for N(1)–C(5)–C(33)–C(38). The two methoxy groups are quasi-coplanar disposition with respect to the phenyl ring as shown by the torsion angle values: C(33)–C(34)–O(39)–C(40) = 165.6(5) and C(33)–C(38)–O(41)–C(42) = −172.8(5)°.

On the other hand, the amidic function is nearly coplanar to the pyrazole ring as shown by the torsion angle N(2)–C(3)–C(17)–N(19) = 28.5(7)°. This planar arrangement results in some close contact between the pyrazole ring and the amidic moiety. The existence of an intramolecular hydrogen bond between N(2) and N(19), [N(2)···N(19) = 2.743(5),

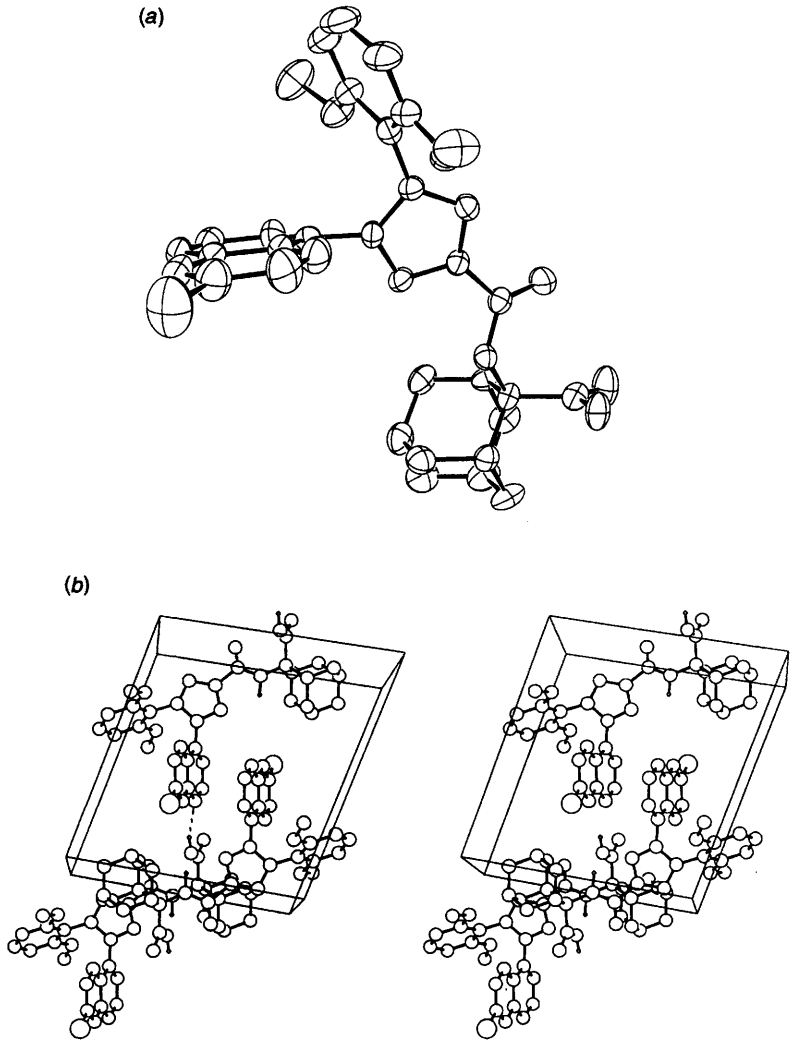

Fig. 1 (*a*) Crystal conformation and (*b*) stereoscopic view of crystal packing of compound **I**. Dotted lines represent intermolecular hydrogen bonds.

Table 2 Main bond lengths (Å) and torsion angles[a] (°) for structure **I** with e.s.d.s in parentheses

N(1)–N(2)	1.357(6)	N(1)–C(5)	1.376(6)
N(1)–C(6)	1.433(6)	N(2)–C(3)	1.328(6)
C(3)–C(4)	1.383(7)	C(4)–C(5)	1.362(7)
C(3)–C(17)	1.495(7)	C(5)–C(33)	1.484(7)
C(17)–O(18)	1.217(6)	C(17)–N(19)	1.353(6)

N(1)–C(5)–C(33)–C(38)	64.8(7)
N(2)–N(1)–C(6)–C(7)	67.3(7)
N(2)–C(3)–C(17)–N(19)	28.5(7)
C(3)–C(17)–N(19)–C(20)	−162.1(5)
C(17)–N(19)–C(20)–C(21) τ_1	−56.7(6)
N(19)–C(20)–C(21)–O(22) τ_2	−59.9(6)
C(33)–C(34)–O(39)–C(40)	165.6(5)
C(33)–C(38)–O(41)–C(42)	−172.8(5)

[a] The opposite torsion angle values are also observed for the reversed conformer (−*x*, −*y*, −*z*).

H(19)···N(2) = 2.236(4) Å, N(19)–H(19)···N(2) = 108.0(2)°], leads to the formation of a virtual five-membered ring N(2)–C(3)–C(17)–N(19)–H(19).

The carboxy moiety presents a *gauche* conformation with the amidic oxygen as shown by the torsion angle C(17)–N(19)–C(20)–C(21) = −56.7(6)°. This kind of disposition is observed for all the NT antagonists we analysed by X-ray diffraction which present an adamantyl group on the C(20) carbon atom.[13]

The crystal packing is mainly governed by intermolecular hydrogen bonds *via* the carboxylic acid function and the nitrogen atoms N(9) [O(22)···N(9) = 2.825(5), H(22)···N(9) = 1.965(4) Å, O(22)–H(22)···N(9) = 161.4(3)°, Fig. 1(*b*)]. The three-dimensional arrangement is also stabilized by π–π interactions, as we can show an aromatic stacking between quinoline rings with a distance (centre to centre) of 3.730 Å [Fig. 1(*c*)].

Isolated state conformation of I

Regarding the conformational restrictions around N(1)–C(6), C(3)–C(17) and C(5)–C(33) bonds,[16] we focused our attention on the less rigid part of compound **I**. Starting from the crystallographic data, we performed semiempirical molecular orbital AM1 calculations in order to scan the conformational space and to determine the lowest energy conformations. This was done by allowing rotations around the $\tau 1$ and $\tau 2$ torsion angles (Scheme 1), *i.e.* the only two single bonds with *a priori* conformational freedom.

The two-dimensional iso-energy contour map presented in Fig. 2 clearly shows a severe conformational restriction around the N(19)–C(20) bond, induced by the presence of the bulky adamantyl group. Concerning the $\tau 1$ torsion angle, a large energy barrier (> 10 kcal mol^{-1}) prevents the rotation towards an *anti* orientation of the carboxylic acid moiety *versus* the amidic carbonyl function. The permitted dispositions are confined to $\tau 1$ values between −80 and 80°, except when the $\tau 2$ values approach 0 or ±180° (Fig. 2).

As observed in the solid state, the two crystalline conformations (X in Fig. 2, ΔE <1 kcal mol^{-1}) are located in the calculated absolute minimum regions.

Structural analysis of II

Single crystal structure of II. The crystal conformation and crystal packing of compound **II** are shown in Fig. 3. Relevant bond lengths and torsion angles are presented in Table 3.

In the same manner, we observe for compound **II** typical bond length values [N(1)–C(6) = 1.43(1) and C(5)–C(30) = 1.48(1) Å] which indicate the absence of any significant orbital overlap[15] between atoms involved in the pyrazole–aromatic ring connection. In accordance with this fact, the quinoline ring and the 2,6-dimethoxyphenyl group are almost perpendicular to the pyrazole ring [N(2)–N(1)–C(6)–C(7) = 114.1(8) and N(1)–C(5)–C(30)–C(35) = 67.3(10) °]. The two methoxy groups

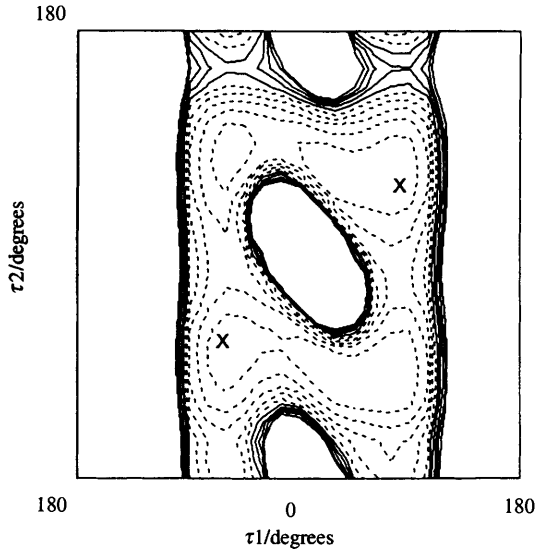

Fig. 2 AM1 conformational iso-energy contour map (ΔE in kcal mol^{-1}; 1 cal = 4.184 J) showing dependence on $\tau 1$ and $\tau 2$ for compound **I**. X corresponds to the crystalline conformation. The contour-to-contour interval is 1 kcal mol^{-1}; dotted lines indicate iso-energies up to 5 kcal mol^{-1} and solid lines, contours from 6 to 10 kcal mol^{-1}.

Table 3 Main bond lengths (Å) and torsion angles (°) for structure **II** with e.s.d.s in parentheses

N(1)–N(2)	1.357(7)	N(1)–C(5)	1.398(10)
N(1)–C(6)	1.432(10)	N(2)–C(3)	1.328(9)
C(3)–C(4)	1.391(10)	C(4)–C(5)	1.360(10)
C(3)–C(17)	1.464(10)	C(5)–C(30)	1.480(10)
C(17)–O(18)	1.222(9)	C(17)–N(19)	1.352(9)

N(1)–C(5)–C(30)–C(35)	−67.3(10)
N(2)–N(1)–C(6)–C(7)	114.1(8)
N(2)–C(3)–C(17)–N(19)	10.7(10)
C(3)–C(17)–N(19)–C(20)	179.9(10)
C(17)–N(19)–C(20)–C(21) τ_1	−132.7(8)
N(19)–C(20)–C(21)–O(22) τ_2	170.7(8)
C(30)–C(31)–O(36)–C(37)	−177.2(7)
C(30)–C(35)–O(38)–C(39)	166.8(7)

are also quasi-coplanar with the phenyl group as shown by the torsion angle values: C(30)–C(31)–O(36)–C(37) = 177.2(7) and C(30)–C(35)–O(38)–C(39) = 166.8(7)°.

The amide function slightly deviates from the plane of the pyrazole ring: N(2)–C(3)–C(17)–N(19) = 10.7(10)°. Such a quasi-planar arrangement partly results in an intramolecular hydrogen bond between N(2) and N(19), [N(2)···N(19) = 2.630(7), H(19)···N(2) = 2.228(7) Å, N(19)–H(19)···N(2) = 154(1)°]. This intramolecular bond leads to the formation of a virtual five-membered ring N(2)–C(3)–C(17)–N(19)–H(19), as was observed for compound **I**.

In the case of compound **II**, however, the carboxy moiety is *anti* to the amidic carbonyl function as shown by the torsion angle C(17)–N(19)–C(20)–C(21) = −132.7(8)°. This conformational difference seems to be directly related to the nature of the substituents around the carbon atom C(20). In a previous study, we generalized this observation by using a statistical analysis of the Cambridge Structural Database.[16] The survey of the conformational behaviour of [CO–NH–C$^{\alpha}$–COOH] torsion angles in organic crystals clearly confirms the idea that the nature of C$^{\alpha}$ (quaternary or tertiary) greatly influences the crystalline conformation of the amino acid.[13] For tertiary C$^{\alpha}$, *anti* and *gauche* conformations occurred equally whereas, in the case of quaternary C$^{\alpha}$, *gauche* conformers are almost exclusively observed.

The chiral carbon atom C(20) is attached to the cyclohexyl group in an equatorial position as generally observed when the cyclohexane substituent is bulky.

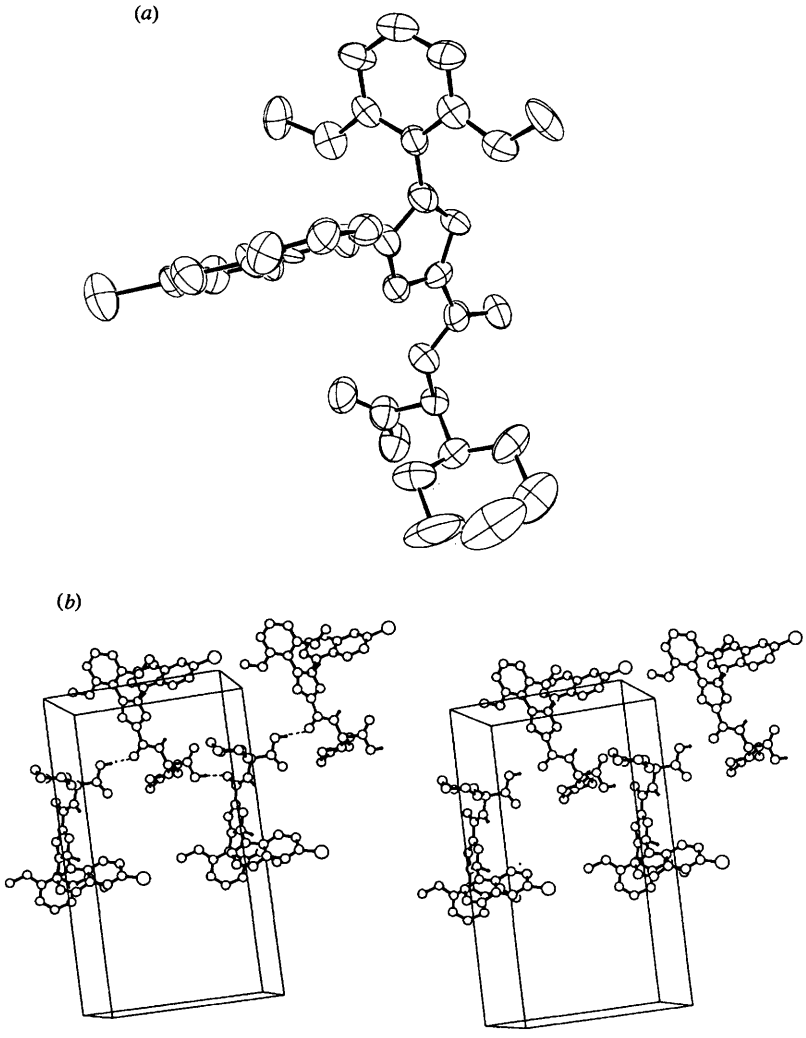

Fig. 3 (*a*) Crystal conformation and (*b*) stereoscopic view of crystal packing of compound **II**. Dotted lines represent intermolecular hydrogen bonds.

The crystal packing is assured by collinear hydrogen bonds between the carboxylic acid function and the amidic oxygen atom O(18) [O(22)···O(18) = 2.610(8), H(22)···O(18) = 1.85(3) Å, O(22)–H(22)···O(18) = 154(1)°, Fig. 3(*b*)], leading to the formation of infinite molecular chains bound together by van der Waals interactions. At this level, we also noticed differences from the crystal packing of compound **I**. Those differences are directly related to steric effects induced by the substituents around the C^{α} carbon atom.

Since those C^{α} substituents play a prominent part in the crystal cohesion (and hence, in biochemical mechanisms) we further investigate the various conformational preferences for compound **II**.

Isolated state conformation of II

In a similar way as for **I**, starting from the crystallographic data, we again performed semiempirical molecular orbital AM1 calculations allowing rotations around $\tau 1$ and $\tau 2$ (Scheme 1).

Compared to compound **I**, the two-dimensional iso-energy contour map (Fig. 4) shows a different pattern, although both compounds have equally potent antagonist activity. The conformational space available for the (*S*) terminal amino-acid is located in negative $\tau 1$ values, while the $\tau 2$ torsion angle varies relatively freely. A large energy barrier (> 10 kcal mol^{-1}), mainly due to steric hindrance, prevents the rotation of the carboxylic acid moiety ($\tau 1$ angle) towards a positive *gauche* orientation of the acid function with respect to the amide carbonyl group, as can be observed for compound **I**. The allowed dispositions are confined in $\tau 1$ values between −170° and 0°, except when the $\tau 2$ values approach 0 or ±180° (Fig. 4). In contrast with compound **I**, the energetically forbidden region for compound **II** is mainly defined by positive $\tau 1$ torsion angle values.

As for the preceding structure, the crystalline state conformation (X in Fig. 4, ΔE < 1 kcal mol^{-1}) is located in a minimum energy well.

Since both molecules are equally active on the NT receptor, we tried to define the common orientation adopted by the acid function in the biological site. For this purpose, we added to the discussion the structural analysis of the inactive compound **III**, the (*R*) enantiomer of **II**. It seems obvious that not only can the bioactive conformation be adopted by the two active analogues (common $\tau 1$–$\tau 2$ torsion angle of low energy), but such conformations have to be energetically forbidden in the case of the inactive enentiomer **III**.

Structural analysis of III

Isolated state conformation of III. For this purpose we used the same method (AM1) as for **I** and **II**. Starting from the crystallographic data of the (*S*) enantiomer, we transformed the relevant torsion angles around the N(19)–C(20) bond to obtain the (*R*) enantiomer **III**. We again performed semiempirical molecular orbital AM1 calculations allowing rotations around $\tau 1$ and $\tau 2$.

The two-dimensional iso-energy contour map is represented in Fig. 5 and corresponds to the inverse of the pattern obtained for compound **II**. The conformational space available for the (*R*) enantiomer **III** is logically located in positive $\tau 1$ values, while the $\tau 2$ torsion angle also varies relatively freely. In con-

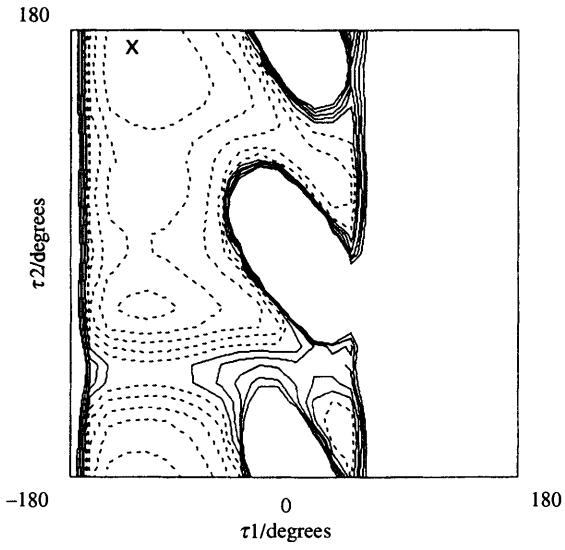

Fig. 4 AM1 conformational iso-energy contour map (ΔE in kcal mol^{-1}) showing dependence on $\tau 1$ and $\tau 2$ for compound **II**. X corresponds to the crystalline conformation. The contour-to-contour interval is 1 kcal mol^{-1}; dotted lines indicate iso-energies up to 5 kcal mol^{-1} and solid lines, contours from 6 to 10 kcal mol^{-1}.

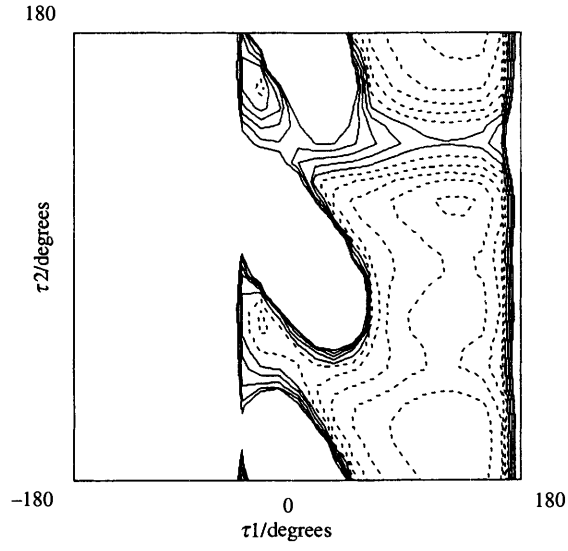

Fig. 5 AM1 conformational iso-energy contour map (ΔE in kcal mol^{-1}) showing dependence on $\tau 1$ and $\tau 2$ for compound **III**. The contour-to-contour interval is 1 kcal mol^{-1}; dotted lines indicate iso-energies up to 5 kcal mol^{-1} and solid lines, contours from 6 to 10 kcal mol^{-1}.

trast with compound **II**, a large energy barrier (> 10 kcal mol^{-1}) prevents the rotation of the carboxylic acid moiety ($\tau 1$ angle) towards a negative *gauche* orientation of the acid function. The low energy conformations of this molecular moiety are principally confined in $\tau 1$ values between 0 and 170°, except when the $\tau 2$ values approach 0 or ±180° (Fig. 5).

Comparison between iso-energy contour maps of compounds I, II and III

According to the energetic criteria described above, we propose in Fig. 6 a graphical representation of putative bioactive conformations for the neurotensin antagonists studied. This figure highlights a conformational area which includes common stable conformations (ΔE < 3 kcal mol^{-1}) for active compounds **I** and **II**, and excludes calculated low energy regions for the inactive enantiomer **III**. We suggest that bioactive conformers have $\tau 1$

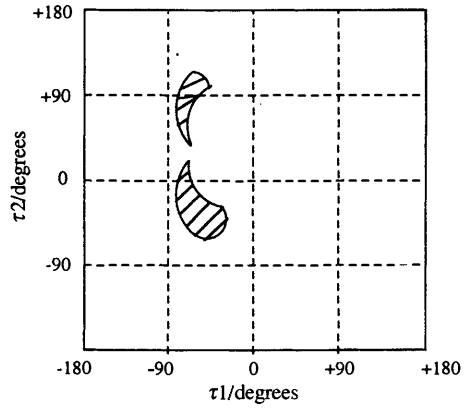

Fig. 6 Graphical representation of putative bioactive conformations ($\tau 1$ and $\tau 2$ torsion angles) for NT antagonists. The shaded area includes common stable conformations (ΔE < 3 kcal mol^{-1}) for active compounds **I** and **II**, and excludes low energy regions of the inactive enantiomer **III**.

torsion angle values of *ca.* −60° and $\tau 2$ values between −60 and +120°.

Molecular superimpositions

Comparison between compounds I, II and III. The crystalline conformation of compound **I** is compatible with our bioactivity hypothesis. Owing to its lack of flexibility, this active compound was taken as the reference for the superposition. Compound **II** was fitted allowing a variation of $\tau 1$ torsion angle value during the flexible molecular superimposition. The observed conformation after superimposition ($\tau 1$ = 56°) is in agreement with our theoretical conclusions for active compounds. Compound **III** was added with $\tau 1$ = 56° by superimposing the two cyclohexyl groups.

The best least-squares molecular superimposition between compounds **I**, **II** and **III** shows that the four pharmacophoric elements {*i.e.* two aromatic moieties—a dimethoxyphenyl ring and a quinoline group, an amidic function [O(18)–C(17)–N(19)] and a bulky lipophilic group, adamantane for **I** and cyclohexyl ring for **II** and **III**} are similarly orientated in those three neurotensin antagonists (Fig. 7). However, the spatial disposition of the carboxylic acid function differentiates active and inactive analogues as shown in Fig. 7.

Conclusions

The present work reports, for the first time, the crystal structure of two potent non-peptide neurotensin antagonists. Common structural features characterize the active molecules. The aromatic moieties are nearly perpendicular to the pyrazole ring. The amidic function slightly deviates from the plane of the pyrazole, by up to 28°, and in both cases we observe an intramolecular hydrogen bond between N(2) and N(19) leading to the formation of a pseudo-five-membered ring. Those molecules appear to be relatively rigid, except for the terminal amino acid part.

At this level, the two analogues show an important conformational difference in the solid state depending on the nature of the substituents around C(20). This difference results in the severe steric restriction induced by the adamantyl ring and greatly influences the crystal packing.

By using computational methods (AM1) and starting from X-ray data, we analysed the conformational properties of compounds **I**, **II** and **III**, in order to differentiate active and inactive analogues. We observe that for active compounds **I** and **II**, the orientations of the carboxylic acid function can be superimposed without any significant increase of energy. However this spatial disposition cannot be reached for compound **III**, due to steric reasons. In conclusion, we suggest that bioactive

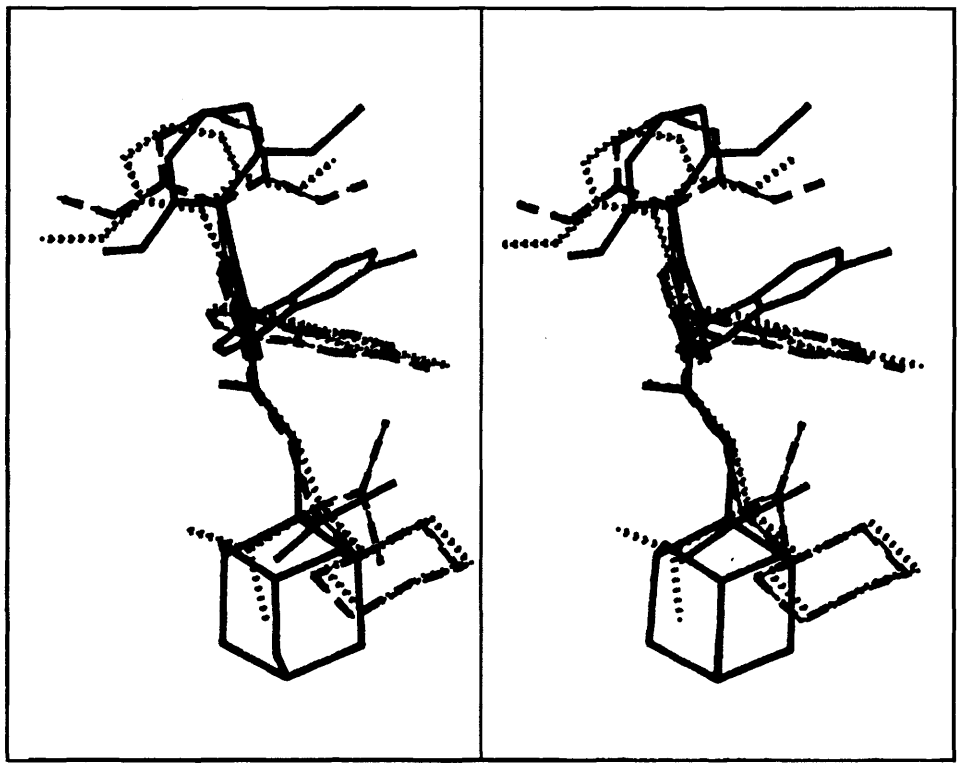

Fig. 7 Stereoscopic view of the best least-squares superimposition between three neurotensin antagonists: **I** (solid line, X-ray crystal structure), **II** (dashed line, X-ray crystal structure except $\tau 1 = -55.8°$), **III** (dotted line, spectral image of compound **II**). This representation shows the orientations of the pharmacophoric elements.

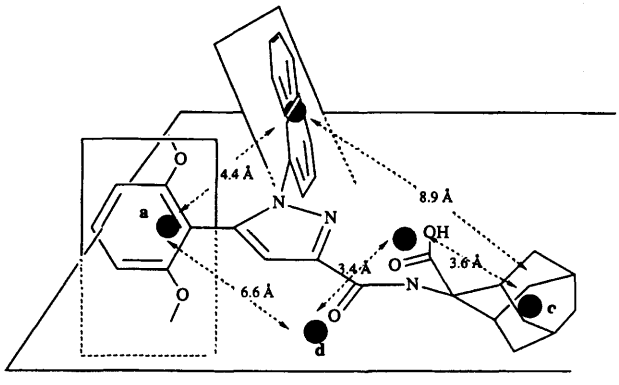

Fig. 8 Pharmacophoric model of neurotensin non-peptide antagonists; (*a*) (centroid of the dimethoxyphenyl group), (*b*) (centroid of the large aromatic moiety), (*c*) (centroid of the adamantane group), (*d*) (amidic oxygen) and (*e*) (centroid of the carboxylic oxygens) represent important pharmacophoric elements; distances between centroids are indicated

conformers have the following common features: $\tau 1$ torsion angle values around $-60°$ and $\tau 2$ values between -60 and $+120°$.

From this information, we have defined a template for potent non-peptide neurotensin receptor antagonists and we propose the first neurotensin antagonist pharmacophoric model (Fig. 8). This work represents a first step toward the modelling of the recognition processes which occur at the binding site.[17]

Experimental

Syntheses

Compounds **I** [2-{[1-(7-chloroquinolin-4-yl)-5-(2,6-dimethoxyphenyl)-1*H*-pyrazol-3-ylcarbonyl]amino}adamantane-2-carboxylic acid], **II** [(*S*)-(+)-{[1-(7-chloroquinolin-4-yl)-5-(2,6-dimethoxyphenyl)-1*H*-pyrazol-3-ylcarbonyl]amino}-cyclohexylacetic acid] and **III** [(*R*)-(−)-{[1-(7-chloroquinolin-4-yl)-5-(2,6-dimethoxyphenyl)-1*H*-pyrazol-3-ylcarbonyl]amino}-cyclohexylacetic acid], were synthesized in the Sanofi Research Laboratories according to a known procedure.[18]

Biochemical tests

The binding assays procedure is as follows.[14] Whole brains (minus cerebellum) were homogenized in 50 mmol dm^{-3} tris·HCl buffer, pH 7.4 with a Polytron (speed 5 for 30 s). After 35 min centrifugation at 30 000 × *g*, the pellet was washed in 50 mmol dm^{-3} tris·HCl buffer, pH 7.4, and resuspended in the same buffer. Binding assays were carried out at 20 °C in 50 mmol dm^{-3} tris·HCl buffer, pH 7.4, containing 0.2% bovine serum albumin, 0.5 mmol dm^{-3} 1,10-phenanthroline and 5 mmol dm^{-3} $MgCl_2$ supplemented with 5 mmol dm^{-3} dithiothreitol and 40 mg dm^{-3} bacitracin, in the presence of 100 pmol dm^{-3} [^{125}I][Tyr^3]neurotensin and membrane proteins (0.3 mg/tube) without or with 1 μmol dm^{-3} levocabastine (Janssen, Beerse, Belgium). Total, non-specific and specific binding were measured at equilibrium (30 min), as previously described, by filtration followed by a wash in tris 50 mmol dm^{-3} bovine serum albumin. IC_{50} values and Hill coefficients were derived from the competition curves obtained with the different unlabelled compounds tested. K_i values were then calculated from corresponding IC_{50} values according to Cheng and Prusoff.[19]

X-Ray crystallography

Crystals of compound **I** were obtained by slow evaporation of an isopropyl alcohol solution at room temperature. A colourless platelet was used for all X-ray measurements. Lattice parameters were obtained from least-squares refinement of the angular settings of 25 well-centred reflections. The X-ray intensities were corrected for Lorentz and polarization effects. The structure was solved by direct methods using SHELX86;[20] the best FOM E map showed all the non-hydrogen atoms. The structure was refined by full-matrix least-squares analysis on *F*

Table 4 Crystallographic data and instrumental setting

	Compound **I**	Compound **II**
Molecular formulae	$C_{32}H_{31}O_5N_4Cl$	$C_{29}H_{29}O_5N_4Cl$
Molecular mass	587.07	549.03
Crystal system	Triclinic	Orthorhombic
Space group	$P\bar{1}$	$P2_12_12_1$
Crystal dimensions/mm	0.22 × 0.10 × 0.03	0.34 × 0.10 × 0.04
a/Å	10.313(2)	13.353(2)
b/Å	11.793(1)	23.900(4)
c/Å	12.669(1)	8.944(1)
α/°	76.458(7)	90
β/°	73.40(1)	90
γ/°	76.180(9)	90
V/Å^3	1410.9(1)	2854.4(7)
Z	2	4
$F(000)$	616	1152
D_c/g cm^{-3}	1.38	1.28
Diffractometer	Enraf-Nonius CAD-4	
Radiation (λ/Å)	Graphite-monochromated Cu-Kα (1.54178)	
$2\theta_{max}$/°	140	130
Unique data	5355 ($-12 \leq h \leq 12$ $-14 \leq k \leq 14$, $-15 \leq l \leq 0$)	4880 ($0 \leq h \leq 15$ $-25 \leq k \leq 28$, $0 \leq l \leq 10$)
Unique data with $I \geq 2\sigma(I)$	2750	2126
Absorpt. coeff./mm^{-1}	1.60	1.54
Final R value	0.06	0.06
Final Rw value	0.07 (Rw) [$w = 1/(\sigma^2(F_o) + 0.001\ F_o^2)$]	0.09 (wR^2) [$w = 1/(\sigma^2(F_o^2) + 0.02\ P)^2$] where $P = (\max(F_o^2,0) + 2F_c^2)/3$
Max. and min. in final diff. Fourier map/e Å^{-3}	0.51 and −0.44	0.18 and −0.14

with the SHELX76 program.[21] Most of the hydrogen atoms (24) appeared in a difference Fourier map but were not refined. 7 H atoms were calculated. Anisotropic thermal parameters were used for all non-H atoms and isotropic ones for H atoms (corresponding to the isotropic thermal parameter of the carrier atom incremented by 0.02). Crystal and refinement data are given in Table 4. The PLATON92 program[22] was used for molecular geometry analysis.

Compound **II** crystallized from a diethylene glycol solution. The crystal structure was obtained using the same procedure as for **I**, except that we used the SHELXL93 program[23] for the refinement. In this case, all of the H atoms were calculated and refined.

Atomic coordinates, bond lengths and angles, and thermal parameters have been deposited at the Cambridge Crystallographic Data Centre (CCDC). For details of the deposition scheme, see 'Instructions for Authors', *J. Chem. Soc., Perkin Trans. 2*, 1996, Issue 1. Any request to the CCDC for this material should quote the full literature citation and the reference number 188/31.

AM1 molecular orbital calculations

The semi-empirical quantum mechanical AM1 method[24] was used in order to scan the conformational space and determine the possible existence of other minima than the ones experimentally observed. Moreover, this method allows us to study the conformational behaviour of compound **III** which was not crystallized. The good performance of this method for conformational analysis problems has been pointed out widely and, moreover, use of more sophisticated methods (*ab initio* calculations) would have been rather time consuming. The two-dimensional (2D) iso-energy contours were built by systematic variation (increment between two successive calculations: 15°, without geometry optimization) using the AM1 option with the standard parameters available within GAUSSIAN92.[25] The starting coordinates, for compounds **I** and **II**, were taken from the X-ray analysis except for the hydrogen atoms placed at standard values depending on the type of carrier atom and hybridization. For compound **III** we used the crystal coordinates of **II** with modifications of dihedral angles values in order to simulate the (*R*)-(+) enantiomer. The 2D iso-contour maps were produced with an in-house device-independent, IBM 9377-90 workstation, contouring program, CPS (Contouring Plotting System),[26] developed in Fortran and using the IBM GRAPHIGS software.[27] Dotted lines indicate iso-energies up to 5 kcal mol^{-1} and solid lines contour from 6 to 10 kcal mol^{-1}. The contour-to-contour interval is 1 kcal mol^{-1}. White zones correspond to energies greater than 10 kcal mol^{-1}. All calculations were performed on the IBM 9377-90 and FPS 264 computer systems of the Scientific Computing Facility Center of the University of Namur.

Molecular superimpositions

Searches for an optimal matching between the various conformations were done using KEMIT[28] developed on the IBM 9377-90 of the Scientific Computing Facility Center of the University of Namur. KEMIT is an in-house device-independent, IBM 6091 workstation, molecular graphics system developed in Fortran and using IBM GRAPHIGS software.[27] Molecular superimpositions are performed by molecular least-squares flexible (*i.e.* allowing rotations around single bonds) or rigid fitting between the cartesian coordinates of particular points (atomic positions in our case) of each molecule using IFMFIT (improved or interactive molecular fiting)[29,30] facility included in KEMIT.

Acknowledgements

The authors are indebted to IBM-Belgique and the *Facultés Universitaires N-D de la Paix* (FNDP, Belgium) for the use of the Namur Scientific Computing Facility. L. Q. thanks B. Norberg and Dr J. Wouters for helpful collaboration.

References

1 R. E. Carraway and S. E. Leeman, *J. Biol. Chem.*, 1973, **248**, 6854.
2 R. E. Carraway and S. E. Leeman, *J. Biol. Chem.*, 1973, **251**, 7045.
3 P. Kitabgi, F. Checler, J. Mazella and J. P. Vincent, *Rev. Basic Clin. Pharmacol.*, 1985, **5**, 397.
4 J. Mai, K. J. Triepel and J. Metz, *Neuroscience*, 1987, **22**, 499.
5 P. Kitabgi and C. B. Nemeroff, *Ann. N. Y. Acad. Sci.*, 1992, **668**, 1.

6 C. B. Nemeroff and S. T. Cain, *Trends Pharmacol. Sci.*, 1985, **6**, 201.
7 P. Kitabgi, *Neurochem. Int.*, 1989, **14**, 111.
8 W. Rostène, A. Brouard, C. Dana, Y. Masuo, F. Agid, M. Vial, A. M. Lhiaubet and D. Pélaprat, *Ann. N. Y. Acad. Sci.*, 1992, **668**, 217.
9 J. F. Liégeois, P. Bonaventure, J. Delarge and J. Damas, *Neurosci. Biobehav. Rev.*, 1995, **19**, 519.
10 J. P. Maffrand, D. Gully, R. Boigegrain, P. Soubrié, P. Kitabgi, W. Rostène and G. Le Fur, *Drugs of the Future*, 1993, **18**, 1137.
11 D. Gully, M. Canton, R. Boigegrain, F. Jeanjean, J. C. Molimard, M. Poncelet, C. Gueudet, M. Heaulme, R. Leyris, A. Brouard, D. Pélaprat, C. Labbé-Jullié, J. Mazella, P. Soubrié, J. P. Maffrand, P. Kitabgi and G. Le Fur, *Proc. Natl. Acad. Sci. USA*, 1993, **90**, 65.
12 J. P. Maffrand, D. Gully, R. Boigegrain and F. Jeanjean, *Proc. XIIIth Int. Symp. Med. Chem.*, Paris, 1994, p. 551.
13 L. Quéré, PhD Thesis, University of Namur, Belgium, L. Quéré et Presses Universitaires de Namur, ISBN: 2 87037 211, 1995.
14 M. Azzi, D. Gully, M. Heaulme, A. Bérod, D. Pélaprat, P. Kitabgi, R. Boigegrain, J. P. Maffrand, G. Le Fur and W. Rostène, *Eur. J. Pharmacol.*, 1994, **255**, 167.
15 F. H. Allen, O. Kennard, D. G. Watson, L. Brammer, A. G. Orpen and R. Taylor, *J. Chem. Soc. Perkin Trans. 2*, 1989, S1–S19.
16 F. H. Allen, O. Kennard and R. Taylor, *Acc. Chem. Res.*, 1983, **16**, 146.
17 L. Quéré, R. Boigegrain, F. Jeanjean, D. Gully, G. Evrard and F. Durant, unpublished work.
18 R. Boigegrain, D. Gully, F. Jeanjean and J. C. Molimard, (Sanofi) EP 0477049 A, 1991.
19 Y. C. Cheng and W. H. Prusoff, *Biochem. Pharmacol.*, 1973, **22**, 3099.
20 G. M. Sheldrick, SHELXS86, Program for Crystal Structure Determinations, University of Göttingen, Federal Republic of Germany, 1986.
21 G. M. Sheldrick, SHELX-76, Program for Crystal Structure Determinations, University of Göttingen, Federal Republic of Germany, 1976.
22 A. L. Spek, *Acta Crystallogr., Sect. A.*, 1990, **46**, C31.
23 G. M. Sheldrick, SHELXL93, Program for Crystal Structure Determinations, University of Göttingen, Federal Republic of Germany, 1993.
24 M. J. S. Dewar, E. G. Zoebisch, E. F. Healy and J. J. P. Stewart, *J. Am. Chem. Soc.*, 1985, **105**, 3902.
25 M. Frisch, G. Trucks, H. Schlegel, P. Gill, B. Johnson, M. Wong, J. Foresman, M. Robb, M. Head-Gordon, E. Replogle, R. Gomperts, J. Andres, K. Raghavachari, J. Binkley, C. Gonzalez, R. Martin, D. Fox, D. Defrees, J. Baker, J. Stewart and J. A. Pople, GAUSSIAN92, Carnegie-Mellon Quantum Chemistry Publishing Unit, Pittsburgh, PA, 1993.
26 G. Baudoux and D. P. Vercauteren, CPS, a contouring plotting system, Facultés Universitaires Notre-Dame de la Paix, Namur, Belgium, 1989.
27 S. Chin, D. P. Vercauteren, W. L. Luken, M. Re, R. Scaneti, R. Tagliavini, D. J. Vanderveken and G. Baudoux, in *Modern Techniques in Computational Chemistry*, MOTECC 89, ed. E. Clementi, ESCOM Publishers, Leiden, 1989, p. 499.
28 D. J. Vanderveken and D. P. Vercauteren, KEMIT, a molecular graphics system, Facultés Universitaires Notre-Dame de la Paix, Namur, Belgium, 1989.
29 J. Lejeune, A. Michel and D. P. Vercauteren, *J. Mol. Graph.*, 1986, **4**, 194.
30 J. Lejeune, A. Michel and D. P. Vercauteren, *J. Comput. Chem.*, 1986, **7**, 739.

Paper 6/03924C
Received 5th *June* 1996
Accepted 5th *August* 1996